

# CSF: Fixed-outline Floorplanning Based on the Conjugate Subgradient Algorithm Assisted by Q-Learning

Xinyan Meng, Huabin Cheng, Rujie Chen, Yu Chen, Wei Zhang, Ning Xu

**Abstract**—To perform the fixed-outline floorplanning problem efficiently, we propose to solve the original nonsmooth analytic optimization model via the conjugate subgradient algorithm (CSA), which is further accelerated by adaptively regulating the step size with the assistance of Q-learning. The objective for global floorplanning is a weighted sum of the half-perimeter wirelength, the overlapping area and the out-of-bound width, and the legalization is implemented by optimizing the weighted sum of the overlapping area and the out-of-bound width. Meanwhile, we also propose two improved variants for the legalization algorithm based on constraint graphs (CGs). Experimental results demonstrate that the CSA assisted by Q-learning (CSAQ) can address both global floorplanning and legalization efficiently, and the two stages jointly contribute to competitive results on the optimization of wirelength. Meanwhile, the improved CG-based legalization methods also outperforms the original one in terms of runtime and success rate.

**Index Terms**—Floorplanning, fixed-outline, nonsmooth optimization, conjugate subgradient algorithm, Q-learning

## I. INTRODUCTION

Floorplanning is a key stage in the physical design flow of very large-scale integration circuit (VLSI) [1]. With the rapid development of integrated circuit manufacturing technology, the complexity of VLSI design has increased dramatically, and modern design usually focuses on fixed-outline floorplanning (FOFP) problems [2]. Compared to layout planning problems without fixed outline, the complexity of the FOFP problem is higher due to the additional constraint of placing a large number of modules within a given outline [3]. Additionally, the usage of intellectual property (IP) core introduces hard modules in the VLSI floorplan, making it much more challenging to optimize the fixed-outline floorplan of mixed-size modules [4].

X. Meng and H. Cheng contributed equally to this work.

X. Meng, R. Chen and Y. Chen are with the School of Mathematics and Statistics, Wuhan University of Technology, Wuhan, 430070, China.

H. Cheng is with the Department of Basic Science, Wuchang Shouyi University, Wuhan, 430064, China.

W. Zhang is with the School of Mathematics and Physics, Wuhan Institute of Technology, Wuhan, 430305, China.

N. Xu is with the school of information engineering, Wuhan University of Technology, Wuhan, 430070, China.

This work is supported in part by the Fundamental Research Funds for the Central University (No. 104972024KFYjc0055), the National Natural Science Foundation of China (No. 92373102,12161039), the Natural Science Foundation of Jiangxi Province (No. 20224BAB201011), and the Foundation of Wuhan Institute of Technology (No. K2024045)

Corresponding authors: Yu Chen (ychen@whut.edu.cn), Wei Zhang (wzhang\_math@whu.edu.cn)

Floorplanning algorithms generally fall into two categories: floorplanning algorithms based on combinatorial optimization model (FA-COM) and floorplanning algorithms based on analytic optimization model (FA-AOM). Coding the relative positions of modules by combinatorial data structures, FA-COM formulates floorplanning problems as combinatorial optimization problems addressed by heuristics or metaheuristics [5]–[8]. Although the combinatorial codes can be naturally converted into compact floorplans complying with the non-overlapping constraint, the combinatorial explosion contributes to their poor performance on large-scale cases. A remedy for this challenge is to implement multilevel methods, in which clustering or partitioning strategies are introduced to reduce the scale of the problem to be addressed [3]. However, the multilevel strategy typically optimizes the floorplan in a local way, which in turn makes it difficult to converge to the globally optimal floorplan of large-scale VLSI designs [9], [10].

FA-AOMs address analytical floorplanning models by continuous optimization algorithms, contributing to their low complexity and fast convergence in large-scale cases [11]. A typical FA-AOM consists of two stages, the global floorplanning stage generating promising results, and the legalization stage that refines the positions of modules to eliminate constraint violations. To get a nice VLSI floorplan, the cooperative design of global floorplanning and legalization is extremely challenging due to the complicated characteristics of floorplanning models. To perform the global floorplanning efficiently, a first-order gradient-based analytic algorithm is typically incorporated to address a smoothed optimization model [12], [13], however, the smoothing approximation could introduce some distortion to the characteristics of the mathematical model. The legalization for the results of global floorplanning can be implemented via the refinement of constraint graphs [12], [13] or the second-order cone programming strategy, which cannot strike a good balance on the time complexity and the minimization of wirelength.

To address the fixed-outline floorplanning problem efficiently, this paper proposes a fixed-outline floorplanning algorithm based on the conjugate subgradient algorithm (CSA), where the Q-learning is introduced to adaptively regulate the step size of CSA. The main contributions of this paper are as follows.

- The nonsmooth wirelength and overlapping metrics are directly optimized by the conjugate subgradient algorithm (CSA). Since the CSA searches the solution space by both the deterministic gradient-based search and the stochastic

exploration, it is much more likely to get the optimal floorplan by flexibly regulating its search step size.

- The CSA step size is dynamically adapted based on Q-learning, which contributes to its fast convergence to optimal floorplan.
- Both global floorplanning and legalization are implemented by the CSA assisted by Q-learning. Consequently, the proposed fixed-outline floorplanning algorithm can strike a balance between time complexity and floorplan quality, and it demonstrates superior stability to the compared algorithms.
- Two improved variants of the CG-based legalization algorithms are proposed. They take less time to get legal floorplans with shorter wirelength.

The remainder of this paper is organized as follows. Section II reviews related work. Section III introduces some preliminaries. Then, the proposed algorithm developed for fixed-outline floorplanning problems is presented in Sections IV. The numerical experiment is performed in Section V to demonstrate the competitiveness of the proposed algorithm, and finally, this paper is concluded in Section VI.

## II. RELATED WORK

By formulating the floorplanning problem as an analytic optimization model, Zhan *et al.* [14] proposed an algorithm framework consisting of the global floorplanning stage and the legalization stage, demonstrating performance superior to the *Parquet-4* based on sequence pair and simulated annealing [3]. Lin and Hung [15] modelled the global floorplanning as a convex optimization problem, where modules are transformed into circles, and a push-pull mode is proposed with consideration of wirelength. Then, a second-order cone programming is deployed to legalize the floorplan. By incorporating the electrostatic field model proposed in *eplace* [16], a celebrated algorithm for standard cell placement in VLSI, Li *et al.* [12] proposed an analytic floorplanning algorithm for large-scale floorplanning cases, and horizontal constraint graphs and vertical constraint graphs were constructed to eliminate overlap of floorplanning results. Huang *et al.* [13] further improved the electrostatics-based analytical method for fixed-outline floorplanning, in which module rotation and sizing were introduced to get floorplanning results with shorter wirelength. Yu *et al.* [17] developed a floorplanning algorithm based on the feasible-seeking approach, achieving better performance than the state-of-the-art floorplanning algorithms.

Since the typical wirelength and overlap metrics of analytical floorplan model are not smooth, additional smoothing approximation must be incorporated to achieve the feasibility of gradient-based optimization algorithms [18]. Popular smoothing approximation methods for the half-perimeter wirelength (HPWL) include the quadratic model, the logarithm-sum-exponential model, and the  $L_p$ -norm model, and the bell-shaped smoothing method is adopted to smooth the overlap metric [18]. In addition, Ray *et al.* [19] proposed a non-recursive approximation to approximate the max function for non-smooth half-perimeter wirelength models, Chan *et al.* [20] employed a Helmholtz smoothing technique to approximate

the density function. However, the additional smoothing process not only introduces extra time complexity of the FA-AOM, but also leads to its local convergence to a solution significantly different from that of the original non-smooth model. Zhu *et al.* [21] proposed to address the non-smooth analytical optimization model of cell placement by the CSA, and Sun *et al.* [22] further developed a CSA-based floorplanning algorithm for scenarios without soft module.

Recently, machine learning (ML) algorithms are introduced to generate general floorplanning algorithms. The generalization ability of well-trained ML algorithms could contribute their potential applications in diverse scenarios of floorplanning, but it is challenging to get an excellent ML-based floorplanning algorithm in the case of inadequate training data. He *et al.* [23] employed agents guided by the Q-learning algorithm, which alleviates the requirement of too much prior human knowledge in the search process. Mirhoseini *et al.* [24] proposed a RL-based method for chip floorplanning, and developed an edge-based graph convolutional neural network architecture capable of learning the transferability of chips. By merging RL with the graph convolutional network (GCN), Xu *et al.* [25] proposed an end-to-end learning-based floorplanning framework named as *GoodFloorplan*. Yang *et al.* [26] proposed an end-to-end reinforcement learning (RL) framework to learn a policy of floorplanning, and promising results are obtained with the assistance of edge-augmented graph attention network, position-wise multi-layer perceptron, and gated self-attention mechanism.

## III. PRELIMINARIES

### A. The Non-smooth Optimization Model of Floorplanning

Let  $\mathbf{x} = (x_1, x_2, \dots, x_n)$  and  $\mathbf{y} = (y_1, y_2, \dots, y_n)$  be the vectors of  $x$ -coordinate and  $y$ -coordinate of all modules, respectively. The fixed-outline floorplanning (FOFP) is to place modules within a fixed outline such that all of them are mutually non-overlapping, formulated as

$$\begin{aligned} \min \quad & W(\mathbf{x}, \mathbf{y}) \\ \text{s.t.} \quad & \begin{cases} D(\mathbf{x}, \mathbf{y}) = 0 \\ B(\mathbf{x}, \mathbf{y}) = 0 \end{cases} \end{aligned} \quad (1)$$

where  $W(\mathbf{x}, \mathbf{y})$ ,  $D(\mathbf{x}, \mathbf{y})$ ,  $B(\mathbf{x}, \mathbf{y})$  are the metrics of wirelength, overlapping and bound excess, respectively. For the global floorplanning stage, we first solve the unconstrained optimization problem

$$\min f_g(\mathbf{x}, \mathbf{y}) = \alpha W(\mathbf{x}, \mathbf{y}) + \lambda D(\mathbf{x}, \mathbf{y}) + \mu B(\mathbf{x}, \mathbf{y}) \quad (2)$$

where  $\alpha$ ,  $\lambda$ , and  $\mu$  are weight coefficients. Then, the legalization is performed by addressing the problem

$$\min f_l(\mathbf{x}, \mathbf{y}) = \lambda D(\mathbf{x}, \mathbf{y}) + \mu B(\mathbf{x}, \mathbf{y}) \quad (3)$$

In (2) and (3), we set  $\mathbf{x}, \mathbf{y} \in \mathbf{R}^n$ . Then, both of them are mixed-variable optimization problems.  $W(\mathbf{x}, \mathbf{y})$ ,  $D(\mathbf{x}, \mathbf{y})$  and  $B(\mathbf{x}, \mathbf{y})$  are defined as follows.

a) *Total Wirelength  $W(\mathbf{x}, \mathbf{y})$* : The total wirelength is here taken as the sum of half-perimeter wirelength (HWPL)

$$W(\mathbf{x}, \mathbf{y}) = \sum_{e \in E} (\max_{v_i \in e} x_i - \min_{v_i \in e} x_i + \max_{v_i \in e} y_i - \min_{v_i \in e} y_i) \quad (4)$$

b) *Sum of Overlapping Area*  $D(\mathbf{x}, \mathbf{y})$ : The sum of overlapping area is computed by

$$D(\mathbf{x}, \mathbf{y}) = \sum_{i,j} O_{i,j}(\mathbf{x}) \times O_{i,j}(\mathbf{y}) \quad (5)$$

where  $O_{i,j}(\mathbf{x})$  and  $O_{i,j}(\mathbf{y})$  represent the overlapping lengths of module  $i$  and  $j$  in the  $X$ -axis and  $Y$ -axis directions, respectively. Denoting  $\Delta_x(i, j) = |x_i - x_j|$ , we know

$$O_{i,j}(\mathbf{x}) = \begin{cases} \min(\hat{w}_i, \hat{w}_j), & \text{if } 0 \leq \Delta_x(i, j) \leq \frac{|\hat{w}_i - \hat{w}_j|}{2} \\ \frac{\hat{w}_i - 2\Delta_x(i, j) + \hat{w}_j}{2}, & \text{if } \frac{|\hat{w}_i - \hat{w}_j|}{2} < \Delta_x(i, j) \leq \frac{\hat{w}_i + \hat{w}_j}{2} \\ 0, & \text{if } \frac{\hat{w}_i + \hat{w}_j}{2} < \Delta_x(i, j) \end{cases} \quad (6)$$

Denoting  $\Delta_y(i, j) = |y_i - y_j|$ , we have

$$O_{i,j}(\mathbf{y}) = \begin{cases} \min(\hat{h}_i, \hat{h}_j), & \text{if } 0 \leq \Delta_y(i, j) \leq \frac{|\hat{h}_i - \hat{h}_j|}{2} \\ \frac{\hat{h}_i - 2\Delta_y(i, j) + \hat{h}_j}{2}, & \text{if } \frac{|\hat{h}_i - \hat{h}_j|}{2} < \Delta_y(i, j) \leq \frac{\hat{h}_i + \hat{h}_j}{2} \\ 0, & \text{if } \frac{\hat{h}_i + \hat{h}_j}{2} < \Delta_y(i, j) \end{cases} \quad (7)$$

where  $\hat{w}_i$  and  $\hat{h}_i$  represent the width and height of module  $i$ .

c) *Sum of Length Beyond the Fixed Outline*  $B(\mathbf{x}, \mathbf{y})$ : For the fixed-outline floorplanning problem, the position of the  $i^{\text{th}}$  module must meet the following constraints:

$$\begin{cases} 0 \leq x_i - \hat{w}_i/2, & x_i + \hat{w}_i/2 \leq W^* \\ 0 \leq y_i - \hat{h}_i/2, & y_i + \hat{h}_i/2 \leq H^* \end{cases}$$

where  $W^*$  and  $H^*$  are the width and the height of fixed-outline, respectively. Let

$$b_{1,i}(\mathbf{x}) = \max_i(0, \hat{w}_i/2 - x_i), b_{2,i}(\mathbf{x}) = \max_i(0, \hat{w}_i/2 + x_i - W^*), \\ b_{1,i}(\mathbf{y}) = \max_i(0, \hat{h}_i/2 - y_i), b_{2,i}(\mathbf{y}) = \max_i(0, \hat{h}_i/2 + y_i - H^*).$$

Accordingly,  $B(\mathbf{x}, \mathbf{y})$  is defined as

$$B(\mathbf{x}, \mathbf{y}) = \sum_{i=1}^n (b_{1,i}(\mathbf{x}) + b_{2,i}(\mathbf{x}) + b_{1,i}(\mathbf{y}) + b_{2,i}(\mathbf{y})) \quad (8)$$

Note that the objective functions in (2) and (3) are not smooth and traditional gradient-based algorithms cannot be applied directly, and we address them by the CSA [21], [22].

### B. The Conjugate Subgradient Algorithm (CSA)

The pseudo code of CSA is presented in Algorithm 1. The iteration process of CSA starts with an initial solution  $\mathbf{u}_0$  and the subgradient  $\mathbf{g}_0$ , and the conjugate direction is initialized as  $\mathbf{d}_0 = \mathbf{0}$ . At generation  $k$ , the searching direction is confirmed according to the subgradient  $\mathbf{g}_k$  and the conjugate direction  $\mathbf{d}_k$ , and the searching step size is determined by dividing a scaling factor  $c$  by the norm of  $\mathbf{d}_k$ . When  $\mathbf{u}$  locates a non-smooth point of  $f$ , the computation of subgradient is performed with a random scheme. Thus, the CSA is not necessarily gradient descendant. Consequently, the adaptive regulation of step size plays a critical role and has a significant influence on its convergence performance, which can be achieved by a reinforcement learning strategy.

### Algorithm 1 CSA

**Input:** Objective function  $f(\mathbf{u})$ , initial solution  $u_0$

**Output:** Optimal solution  $\mathbf{u}^*$

- 1: Set  $\mathbf{g}_0 \in \partial f(\mathbf{u}_0)$ ,  $\mathbf{d}_0 = \mathbf{0}$ ;
- 2: **for**  $k = 1$  to  $k_{max}$  **do**
- 3:   Calculate the subgradient  $\mathbf{g}_k \in \partial f(\mathbf{u}_{k-1})$ ;
- 4:   Calculate the *Polak-Ribiere* parameter  $\eta_k = \frac{\mathbf{g}_k^T(\mathbf{g}_k - \mathbf{g}_{k-1})}{\|\mathbf{g}_{k-1}\|_2^2}$ ;
- 5:   Calculate the conjugate direction  $\mathbf{d}_k = -\mathbf{g}_k + \eta_k \mathbf{d}_{k-1}$ ;
- 6:   Calculate the step size  $\hat{a}_k = \frac{c}{\|\mathbf{d}_k\|_2}$ ;
- 7:   Update the solution  $\mathbf{u}_k = \mathbf{u}_{k-1} + \hat{a}_k \mathbf{d}_k$ ;
- 8:   Update the optimal solution  $\mathbf{u}^*$ ;
- 9: **end for**

### C. Q-learning

We propose to update the scaling parameter  $c$  in Algorithm 1 by Q-learning, a typical value-based reinforcement learning algorithm [27]. Its goal is to find for each state-action pair  $(s, a)$  a Q-value that represents its long-term expected return. The Q-values record an individual's learning experience, stored in a Q-table and updated by

$$Q^k(s_j, a_i) = (1 - \alpha_0)Q^{k-1}(s_j, a_i) + \alpha_0(R(s_j, a_i) + \gamma_0 Q_{max}), \quad (9)$$

where  $Q^k(s_j, a_i)$  represents the Q-values of the state-action pair  $(s_j, a_i)$  at steps  $k$ .  $\alpha_0$ ,  $\gamma_0$  are the learning rate and the discount rate, and  $R(s_j, a_i)$  is the reward function. In this paper,  $Q_{max}$  is confirmed as

$$Q_{max} = m_0 Q^{k-1}(s_j, a_i) + \frac{1 - m_0}{p - 1} \sum_{l \neq j}^p Q_{max}^{k-1}(s_l), \quad (10)$$

where  $m_0$  is a preset coefficient.  $Q_{max}^{k-1}(s_l)$  is the maximum Q-value in all actions of state  $l$  in the previous iteration.

### D. The Constraint Graph

The constraint graph (CG) is a directed acyclic graph (DAG) used to represent the relative position among various modules in a layout. Modules are represented by vertexes of a CG, and arcs indicate the constraint relationships between modules. Accordingly, the horizontal constraint graph (HCG) and the vertical constraint graph (VCG) are constructed, which are composed of a series of arcs to show the positional relationships left-right and down-up between modules, respectively. Given a floorplan of modules, the HCG and the VCG can be constructed by visiting all modules. If the lower left corner coordinates of module  $A$  are less than those of module  $B$ , then the arcs of the HCG and the VCG are constructed in the following way [12]:

- 1) If module  $A$  and  $B$  do not overlap in either horizontal or vertical direction, then add the arc  $A \rightarrow B$  in the HCG and add the arc  $A \uparrow B$  in the VCG.
- 2) If module  $A$  and  $B$  overlap in the vertical direction but not in the horizontal direction, then add the arc  $A \rightarrow B$  in the HCG; add the arc  $A \uparrow B$  in the VCG if module  $A$  and  $B$  overlap in the horizontal direction but not in the vertical direction.
- 3) For the case that module  $A$  and  $B$  overlap in both horizontal and vertical directions, add the arc  $A \uparrow B$

in the VCG if the overlapping length in the horizontal direction is greater than that in the vertical direction; conversely, add the arc  $A \rightarrow B$  in the HCG.

It is worth mentioning that a properly constructed CG pair (HCG, VCG) can be directly used to translate into a floorplan where all modules are mutually disjoint.

#### IV. THE CSA-BASED FIXED-OUTLINE FLOORPLANNING ALGORITHM

As presented in Section III-A, the stages of global floorplanning and legalization can be implemented by addressing (2) and (3), respectively. Due to the non-smooth characteristics, we propose a CSA-based fixed-outline floorplanning algorithm (CSF). In the CSF, the non-smooth optimization problems (2) and (3) are addressed by CSA [22]. Meanwhile, we also improve the performance of CSA by adaptively regulating the scaling factor of step size via Q-learning.

##### A. The Framework of CSF

The framework of CSF is illustrated by Algorithm 2. At the beginning, a solution population  $Pop$  is initialized, where the orientations of modules are randomly selected and the latin hypercube sampling (LHS) is employed to generate the initial position of the module  $fp_j$  for each individual  $ind_i$  in the solution population [22],  $p$  and  $N$  represent the population size and the total number of modules respectively. The characteristic of LHS lies in that it can make the generated samples distribute as evenly as possible in the parameter space, thus covering a broader solution space and being more likely to find the global optimal solution. Then, the stages of global floorplanning and legalization are successively implemented. If a legal solution  $\mathbf{FP}^*$  is obtained after the legalization stage, record this solution as the final solution and terminate the iteration. Otherwise, some randomly selected modules are rotated and the floorplanning process can be repeated again until the iteration budget is exhausted.

---

##### Algorithm 2 The framework of CSF

---

**Input:** Iteration buget  $t_{max}$ ;

**Output:** Legal floorplan  $\mathbf{ind}^* = (\mathbf{fp}_1, \dots, \mathbf{fp}_N)$ ;

- 1: Generate  $\mathbf{ind}_i = (\mathbf{fp}_1, \dots, \mathbf{fp}_N)$  ( $i = 1, \dots, p$ ) by LHS;
  - 2: Set  $t = 1$ ;
  - 3: **while**  $t < t_{max}$  **do**
  - 4:   Implement global floorplanning by addressing (2);
  - 5:   Implement legalization by addressing (3);
  - 6:   **if** the solution  $\mathbf{FP}^*$  obtained after legalization is legal **then**
  - 7:     Set  $\mathbf{ind}^* = \mathbf{FP}^*$ ;
  - 8:     **break**;
  - 9:   **end if**
  - 10:   Rotate selected modules of  $\mathbf{ind}_i$  ( $i = 1, \dots, p$ );
  - 11:   **++**;
  - 12: **end while**
- 

##### B. The Conjugate Subgradient Algorithm Assisted by Q-learning

To address the fixed-outline floorplanning problem efficiently, we propose a conjugate subgradient algorithm assisted by Q-learning (CSAQ), which employs a population-based iteration scheme with the principle of CSA. Thanks to the gradient-like definition and the stochastic characteristics of subgradient, the CSA incorporates both the fast convergence of gradient-based algorithm and the global convergence of meta-heuristics. The step size controlled by  $c$  plays a crucial role in achieving the balance between exploration and exploitation.

Because appropriate behaviors make it easier for individuals to find the optimal strategy to obtain the maximum long-term return [28], we employ a dynamical update strategy of  $c$  using a Q-learning-assisted strategy [29].

1) *The Q-learning strategy:* For a population of size  $p$ , a  $p \times m$  Q-table is constructed as Table I, where each state corresponds to an individual, and  $m$  actions represent the update strategies of  $c$  [29]. Then, the scaling factor  $c$  is updated for state  $s_j$  according to the probability distribution

$$P_i^j = \frac{Q^k(s_j, a_i)}{\sum_{l=1}^m Q^k(s_j, a_l)}, i = 1, \dots, m, \quad (11)$$

where  $Q^k(s_j, a_i)$  represents the Q-value of state-action pair  $(s_j, a_i)$  at the  $k$ -th iteration. At each iteration, the Q-values are updated by (9) and the reward function  $R(s_j, a_i)$  is confirmed by .

$$R(s_j, a_i) = (f_{pre} - f_{post})/100, \quad (12)$$

where  $f_{pre}$  and  $f_{post}$  are the pre-action value and the post-action value of the objective function  $f$  to be minimized.

TABLE I: The Q-table for the update of  $c$ .

State	Action			
	$a_1$	$a_2$	...	$a_m$
$s_1/\mathbf{ind}_1$	$Q(s_1, a_1)$	$Q(s_1, a_2)$	...	$Q(s_1, a_m)$
$s_2/\mathbf{ind}_2$	$Q(s_2, a_1)$	$Q(s_2, a_2)$	...	$Q(s_2, a_m)$
...	...	...	...	...
$s_p/\mathbf{ind}_p$	$Q(s_p, a_1)$	$Q(s_p, a_2)$	...	$Q(s_p, a_m)$

2) *The framework of CSAQ:* With the probability distribution confirmed by (11), the parameter  $c$  is updated every  $k_t$  generation. Accordingly, we get the framework of CSAQ as presented in Algorithm 3.

##### C. The Global Floorplanning Stage

The global floorplanning stage is implemented by addressing problem (2) using the CSAQ described by Algorithm 3. The motivation is to get properly distributed modules by minimizing the penalized objective with increasing  $\lambda$ . The iteration process ceases if the total overlapping area of all individuals in the solution population is less than  $A/v$ , where  $A$  is the sum of the areas of all modules and  $v$  is a preset constant. The process of global floorplanning is shown in Algorithm 4.

---

**Algorithm 3** CSAQ
 

---

**Input:** The objective  $f$ , the population  $\mathbf{Pop} = \{\mathbf{ind}_j, j = 1, \dots, p\}$ , the iteration gap  $k_t$ , the initial parameter  $c$ ;  
**Output:** The updated solution population  $\mathbf{Pop}$ ;

- 1: Initialize the Q-table (Table I) uniformly;
- 2: **for**  $k = 1$  to  $k_{max}$  **do**
- 3:   **for**  $j = 1$  to  $p$  **do**
- 4:     **if**  $k == 1$  **then**
- 5:       Set  $R(s_j, a_i) = 0$  for all  $i \in \{1, \dots, m\}$ ;
- 6:        $\mathbf{d}_{j,0} = \mathbf{0}$ ,  $\mathbf{ind}_j^0 = \mathbf{ind}_j$ ,  $\mathbf{g}_{j,0} \in \partial f(\mathbf{ind}_j^0)$ ;
- 7:     **end if**
- 8:     **if**  $k \pmod{k_t} = 0$  **then**
- 9:       Update  $Q^k(s_j, a_i)$  according to (9);
- 10:       Update  $c_j$  according to (11);
- 11:     **end if**
- 12:     Calculate the subgradient  $\mathbf{g}_{j,k} \in \partial f(\mathbf{ind}_j^{k-1})$ ;
- 13:     Calculate the parameter  $\eta_{j,k} = \frac{\mathbf{g}_{j,k}^T(\mathbf{g}_{j,k} - \mathbf{g}_{j,k-1})}{\|\mathbf{g}_{j,k-1}\|_2^2}$ ;
- 14:     Calculate the conjugate direction  $\mathbf{d}_{j,k} = -\mathbf{g}_{j,k} + \eta_{j,k}\mathbf{d}_{j,k-1}$ ;
- 15:     Calculate the step size  $\hat{a}_{j,k} = \frac{c_j}{\|\mathbf{d}_{j,k}\|_2}$ ;
- 16:     Update the solution  $\mathbf{ind}_j^k = \mathbf{ind}_j^{k-1} + \hat{a}_{j,k}\mathbf{d}_{j,k}$ ;
- 17:   **end for**
- 18: **end for**
- 19: **Set**  $\mathbf{Pop} = \{\mathbf{ind}_j^{k_{max}}, j = 1, \dots, p\}$ .

---



---

**Algorithm 4** Global Floorplanning by the CSAQ
 

---

**Input:** The objective  $f_g$ , the population  $\mathbf{Pop} = \{\mathbf{ind}_1, \dots, \mathbf{ind}_p\}$ ;  
**Output:** The updated solution population  $\mathbf{Pop}^*$ ;

- 1: Initialize parameters  $\alpha$ ,  $\lambda$  and  $\mu$  of the objective  $f_g$ ;
- 2: **while** the termination condition is not met **do**
- 3:   Perform Algorithm 3
- 4:   **for**  $j = 1$  to  $p$  **do**
- 5:      $\mathbf{ind}_j = \mathbf{ind}_j^{k_{max}}$ ;
- 6:   **end for**
- 7:   Set  $\lambda = q * \lambda$ ;
- 8: **end while**
- 9: **Pop** $^* = \{\mathbf{ind}_1, \dots, \mathbf{ind}_p\}$ .

---

#### D. The Legalization Stage

After the global floorplanning stage, a legalization procedure is implemented to get a legal floorplan. In this paper, we propose two legalization strategies, the improved legalization based on the constraint graphs and the legalization based on the CSAQ.

1) *Legalization based on the constraint graphs:* The legalization based on the constraint graph starts with the construction of the HCG and the VCG. Then, the coordinates of the modules are renewed according to the constructed constraint graphs. If all modules are placed in the constrained region, we get the final floorplan. Otherwise, additional strategies are employed to get a legal floorplan. The process of eliminating out-of-bound aims to adjust a constraint relationship in the critical path of a CG. Since the process to eliminate horizontal bound excess is similar to that in the vertical direction, we only present the details of horizontal legalization.

Li *et al.* [12] proposed a CG-based legalization for large-scale floorplanning, where a critical relationship  $A \rightarrow B$  is removed from the HCG, and a corresponding relationship is added to the VCG if it is needed. According to Li's legalization algorithm, the modification of HCG is implemented as follows.

- 1) If  $A \rightarrow B$  is *compressible*, it is removed from the HCG.
- 2) The critical relationship with the maximum *weight* is removed from the HCG, and a corresponding relationship is inserted to the VCG at the same time. The weight of  $A \rightarrow B$  is computed by

$$weight(A \rightarrow B) = \begin{cases} S_A^y - h_B & \text{if } y_A \leq y_B, \\ S_B^y - h_A & \text{otherwise,} \end{cases} \quad (13)$$

where  $S_A^y$  and  $S_B^y$  are the respective vertical slacks of modules  $A$  and  $B$ .

Although modification of the critical relationship with the maximum weight can reduce the vertical placement range to the greatest extent, it is sometimes not the best choice in terms of wirelength. Accordingly, we propose an improved legalization strategy ( $ILG_x$ ) as presented in Algorithm 5.

---

**Algorithm 5**  $ILG_x(W, HCG, VCG)$ 


---

**Input:** Width  $W$  of the fixed outline, horizontal and vertical constraint graphs ( $HCG, VCG$ );  
**Output:** ( $HCG, VCG$ ) after horizontal legalization.

- 1: Calculate the width  $W_d$  of the current floorplan and locate all the critical relationships in the  $HCG$ ;
- 2: **while**  $W_d > W$  **do**
- 3:   **if** there exists a *compressible*  $A \rightarrow B$  **then**
- 4:     Remove  $A \rightarrow B$  from the HCG;
- 5:   **else**
- 6:     Calculate the weights of all critical relationships by (13);
- 7:     Select critical relationships  $\{A_i \rightarrow B_i, i = 1, \dots, k\}$  with  $k$  greatest weights;
- 8:     Calculate the selection probability  $Pw_i$  for  $A_i \rightarrow B_i$  ( $i = 1, \dots, k$ );
- 9:     Set  $A \rightarrow B$  as a relationship selected from  $\{A_i \rightarrow B_i, i = 1, \dots, k\}$  according to the distribution  $\{Pw_i, i = 1, \dots, k\}$ ;
- 10:    Remove  $A \rightarrow B$  from the HCG;
- 11:    **if**  $y_A \leq y_B$  **then**
- 12:      Insert  $A \uparrow B$  to the VCG;
- 13:    **else**
- 14:      Insert  $B \uparrow A$  to the VCG;
- 15:    **end if**
- 16:    **end if**
- 17:    Calculate the width  $W_d$  and locate all critical relationships in the  $HCG$ ;
- 18: **end while**

---

According to the weight values, the proposed  $ILG_x$  sorts all incompressible relationships in descending order, and then selects  $k$  of them with the greatest values as the candidate relationships. To select one of the  $k$  candidate relationships to be removed from the  $HCG$ , we estimate the wirelength changes of the potential removals, and sort them in descending order of wirelength change. Then, we establish a probability distribution  $\{Pw_i, i = 1, \dots, k\}$ , where  $Pw_i > Pw_{i+1}$  for  $i = 1, \dots, k-1$ . In this way, the legalization of floorplan can lead to shorter total wirelength.

The vertical legalization  $ILG_y$  can be carried out in similar way. By alternatively executing  $ILG_x$  and  $ILG_y$  until a legal floorplan is obtained or the maximum number of iterations  $l_{max}$  is reached, we get the improved legalization algorithm based on constraint graphs presented in Algorithm 6.

---

**Algorithm 6** Improved Legalization by the CGs
 

---

**Input:**  $W, H$ , the solution  $\mathbf{FP} = (\mathbf{fp}_1, \dots, \mathbf{fp}_N)$  to be legalized, the maximum number of iterations  $l_{max}$ ;  
**Output:** The updated solution  $\mathbf{FP}^* = (\mathbf{fp}_1^*, \dots, \mathbf{fp}_N^*)$ ;  
 1: Generate  $HCG$  and  $VCG$  according to  $\mathbf{FP}$ ;  
 2: Update  $\mathbf{FP}$  according to the  $HCG$  and the  $VCG$ ;  
 3: **for**  $i = 1$  to  $l_{max}$  **do**  
 4:   Perform  $ILG_x$  to update  $\mathbf{FP}$ ;  
 5:   Perform  $ILG_y$  to update  $\mathbf{FP}$ ;  
 6:   **if**  $\mathbf{FP}$  is legal **then**  
 7:      $\mathbf{FP}^* = \mathbf{FP}$ ;  
 8:     **break**;  
 9:   **end if**  
 10: **end for**

---

2) *Legalization based on the CSAQ*: Sun *et al.* [22] proposed to optimize (3) by CSA to get a legal floorplan. To improve the performance of CSA-based legalization, the CSA-Q is employed in this paper to address problem (3). As presented in Algorithm 7, the CSAQ used in the legalization stage is similar to that deployed in the global floorplanning stage, and the iteration process is terminated when either the maximum number of iterations is reached or a legal individual (floorplan) is obtained. Since the legalization process based on CSAQ sometimes gets an incompact floorplan, the constraint graphs are finally constructed to update the legalized floorplan to get a compact one.

## V. EXPERIMENTAL RESULTS

To verify the competitiveness of the proposed algorithm CSF, we perform numerical experiments on the GSRC and MCNC benchmarks. The I/O pads are fixed at the given coordinates for all of the test circuits, and all modules are set as hard modules. The algorithm is implemented in C++ and run on a 64-bit Windows laptop with 2.4 GHz Intel Core i7-13700H and 16-GB memory. The wirelength was evaluated by HPWL for all test cases. The aspect ratio  $R$  is set as 1, unless otherwise specified, the  $\gamma = 15\%$  and the width and height are generated by

$$W = \sqrt{(1 + \gamma) \cdot A/R}, \quad H = \sqrt{(1 + \gamma) \cdot A \cdot R}. \quad (14)$$

### A. The Positive Function of Q-learning

In the proposed CSAQ, the Q-learning strategy is introduced to automatically regulate the scale factor  $c$  of the CSA. The adaptive regulation of  $c$  contributes to better convergence of CSA in both the global floorplanning stage and the legalization stage.

#### 1) The performance of CSAQ-based global floorplanning:

To validate the performance improvement of CSAQ introduced by the Q-learning strategy, we compare two variants of CSF, 1) the CSF-cc implementing both global floorplanning and legalization by CSA and 2) the CSF-qc implementing global floorplanning and legalization by CSAQ and CSA, respectively. Due to the random characteristics of CSA, the performances are compared by averaged results of 30 independent runs. The average runtime of a single run of global floorplanning ( $t_g$ ),

---

**Algorithm 7** Legalization by the CSAQ
 

---

**Input:** The Objective  $f_l$ , the population  $\mathbf{Pop} = \{\mathbf{ind}_1, \dots, \mathbf{ind}_p\}$ ;  
**Output:** The updated solution  $\mathbf{FP}^* = (\mathbf{fp}_1^*, \dots, \mathbf{fp}_N^*)$ ;  
 1: Initialize parameters  $\lambda$  and  $\mu$  of the objective  $f_l$ , set  $\text{succ}=0$ , initialize the Q-table (Table I) uniformly;  
 2: **for**  $k = 1$  to  $k_{max}$  **do**  
 3:   **for**  $j = 1$  to  $p$  **do**  
 4:     **if**  $k == 1$  **then**  
 5:       Set  $R(s_j, a_i) = 0$  for all  $i \in \{1, \dots, m\}$ ;  
 6:        $\mathbf{d}_{j,0} = \mathbf{0}$ ,  $\mathbf{ind}_j^0 = \mathbf{ind}_j$ ,  $\mathbf{g}_{j,0} \in \partial f(\mathbf{ind}_j^0)$ ;  
 7:     **end if**  
 8:     **if**  $k \pmod{k_t} = 0$  **then**  
 9:       Update  $Q^k(s_j, a_i)$  according to (9);  
 10:       Update  $c_j$  according to (11);  
 11:     **end if**  
 12:     Calculate the subgradient  $\mathbf{g}_{j,k} \in \partial f(\mathbf{ind}_j^{k-1})$ ;  
 13:     Calculate the parameter  $\eta_{j,k} = \frac{\mathbf{g}_{j,k}^T (\mathbf{g}_{j,k} - \mathbf{g}_{j,k-1})}{\|\mathbf{g}_{j,k-1}\|_2^2}$ ;  
 14:     Calculate the conjugate direction  $\mathbf{d}_{j,k} = -\mathbf{g}_{j,k} + \eta_{j,k} \mathbf{d}_{j,k-1}$ ;  
 15:     Calculate the step size  $\hat{a}_{j,k} = \frac{c_j}{\|\mathbf{d}_{j,k}\|_2}$ ;  
 16:     Update the solution  $\mathbf{ind}_j^k = \mathbf{ind}_j^{k-1} + \hat{a}_{j,k} \mathbf{d}_{j,k}$ ;  
 17:     **if**  $\mathbf{ind}_j^k$  is legal **then**  
 18:        $\text{succ}=1$ ,  $\mathbf{FP}^* = \mathbf{ind}_j^k$ ;  
 19:       **Break**;  
 20:     **end if**  
 21:   **end for**  
 22:   **if**  $\text{succ}=1$  **then**  
 23:     **Break**;  
 24:   **end if**  
 25: **end for**  
 26: Update  $\mathbf{FP}$  by the constraint graphs to get tight floorplans.

---

the average runtime of a single run of legalization ( $t_l$ ), the average runtime of floorplanning ( $t_w$ ), the success rate (SR) and the average wirelength (HPWL) are included in Table II. We further perform a one-side Wilcoxon rank-sum test for the optimization results of wirelength, and the p-values and the test results (R) with a significance level of 0.05 are also demonstrated in Table II, where “+” indicates that CSF-qc significantly outperforms CSF-cc and “~” means that the difference is not significant.

Compared with the CSF-cc, where CSA is not equipped

TABLE II: Performance comparison between CSA-based and CSAQ-based global floorplanning.

Circuit	Method	Runtime			SR(%)	HPWL( $\mu\text{m}$ )	p-value	R
		$t_g$ (s)	$t_l$ (s)	$t_w$ (s)				
ami33	CSF-cc	0.19	0.41	<b>0.72</b>	73.3	133702	0.09	~
	CSF-qc	0.81	0.53	1.61	<b>93.3</b>	<b>131427</b>		
ami49	CSF-cc	0.13	0.08	<b>0.35</b>	96.6	<b>916042</b>	0.11	~
	CSF-qc	0.41	0.10	0.65	<b>100</b>	924246		
n100	CSF-cc	0.22	0.07	<b>0.35</b>	100	293202	0.24	~
	CSF-qc	1.35	0.06	1.52	100	<b>292880</b>		
n200	CSF-cc	0.63	0.13	<b>0.82</b>	100	524905	0.03	+
	CSF-qc	4.27	0.18	4.62	100	<b>523229</b>		
n300	CSF-cc	1.47	0.34	<b>1.98</b>	100	595735	0.28	~
	CSF-qc	10.89	0.16	11.05	100	<b>593784</b>		

with Q-learning, the CSF-qc also achieves an improved success rate on the MCNC benchmarks at the expense of a bit longer runtime. It also demonstrates that the better floorplanning results obtained by CSAQ can even shorten the runtime of legalization implemented by CSA. Although the Q-learning strategy is only introduced in the global floor planning stage, it is still effective in terms of the average wirelength of the final floorplan. However, the positive influence on the legalized floorplan is not very significant for the benchmarks except for the “n200” case.

2) *The performance of CSAQ-based legalization:* The CSF-qc is further compared with the CSF-qq, where both global floorplanning and legalization are implemented by addressing (3) via CSAQ, and the results are included in Table III.

TABLE III: Performance comparison between CSA-based and QCSA-based legalization.

Circuit	Method	Runtime			SR(%)	HPWL( $\mu\text{m}$ )	p-value	R
		$t_g(s)$	$t_l(s)$	$t_w(s)$				
ami33	CSF-qc	0.81	0.53	<b>1.61</b>	93.3	131427	$4.79 \times 10^{-11}$	+
	CSF-qq	0.75	0.98	1.88	<b>100</b>	<b>84427</b>		
ami49	CSF-qc	0.41	0.10	<b>0.65</b>	100	924246	0.21	-
	CSF-qq	0.45	0.26	0.78	100	<b>902566</b>		
n100	CSF-qc	1.35	0.06	<b>1.52</b>	100	292880	$7.92 \times 10^{-5}$	+
	CSF-qq	1.33	0.25	1.68	100	<b>290207</b>		
n200	CSF-qc	4.27	0.18	<b>4.62</b>	100	523229	$9.30 \times 10^{-7}$	+
	CSF-qq	4.28	0.64	5.25	100	<b>519860</b>		
n300	CSF-qc	10.89	0.16	<b>11.05</b>	100	593784	$4.76 \times 10^{-4}$	+
	CSF-qq	11.21	0.92	12.13	100	<b>588951</b>		

The results show that by employing the Q-learning strategy, the CSAQ leads to significantly better legalization results of the investigated benchmarks. The statistical test indicates that CSF-qq performs significantly better than CSF-qc on 4 of 5 problems. Although the test does not demonstrate significant superiority of CSF-qq in the *ami49* case, it still beats CSF-qc in terms of the average wirelength.

### B. Performance comparison of legalization algorithms

Li *et al.* [12] proposed a CG-based legalization algorithm (LA) for large-scale fixed-outline floorplanning, and an improved variant (ILA) is proposed by us in Algorithm 6 to further refine the results of wirelength optimization. Motivated by the idea of legalizing the floorplan by addressing a nonsmooth optimization problem [22], we also proposed a CSAQ-based legalization algorithm (CLA) presented by Algorithm 7. To compare their performance, we generate the initial floorplan to be legalized by the CSAQ-based global floorplanning algorithm presented in Algorithm 4.

Note that the ILA involves a parameter  $k$  that determines the number of candidate correction relationships to be selected probabilistically. In our experiments, we get two variants of ILA by setting  $k = 3$  with two probability distributions.

- ILAm:  $Pw_1 = 0.9$ ,  $Pw_2 = 0.05$ ,  $Pw_3 = 0.05$ ;
- ILAs:  $Pw_1 = 1$ ,  $Pw_2 = 0$ ,  $Pw_3 = 0$ .

For each benchmark problem, the white space is set to 20%, and 30 independent experiments are performed to get the statistical results presented in TABLE IV, where MinW and HWS D represent the minimum value and the standard deviation of the results of 50 independent runs, respectively.

The results show that the improved CG-based legalization algorithms (ILAm and ILAs) generally outperform the LA

TABLE IV: Comparison of Different legalization Methods

Circuit	Method	HPWL( $\mu\text{m}$ )	MinW( $\mu\text{m}$ )	CPU(s)	SR(%)	HWS D( $\mu\text{m}$ )
ami33	LA [12]	116384	89851	0.51	90	14852.88
	ILAm	109153	86236	0.17	100	10306.27
	ILAs	101496	86147	0.63	100	11993.17
	CLA	83452	75783	0.08	100	5383.99
ami49	LA [12]	1563721	980543	0.33	96	253380.55
	ILAm	1304216	921645	0.29	96	252591.71
	ILAs	1292577	894563	1.04	90	181419.36
	CLA	917899	806937	0.15	100	62604.82
n100	LA [12]	335610	310834	3.64	100	18157.76
	ILAm	314903	286532	2.42	100	14945.68
	ILAs	305016	286748	2.84	100	12775.31
	CLA	290495	286277	1.42	100	2273.33
n200	LA [12]	636552	538590	22.22	100	29538.32
	ILAm	568583	513892	12.17	100	22937.34
	ILAs	560880	515428	12.67	100	25125.83
	CLA	520160	516038	4.61	100	2391.86
n300	LA [12]	806155	588942	66.30	100	53314.69
	ILAm	667439	581653	42.37	100	22937.34
	ILAs	636666	583300	38.87	100	30192.93
	CLA	591151	581712	11.29	100	4667.06

in terms of both the average wirelength and the minimum wirelength. Since ILAs always selects the candidate correction relationship with the smallest wirelength, it optimizes the wirelength better than ILAm. However, the heuristic selection strategy of ILAs sometimes leads to unpromising local convergence of the legalization process, resulting in a lower success rate for the *ami49* circuit. Compared with the CG-based legalization methods including LA, ILAm and ILAs, the CLA can get legalized floorplans with the shorter wirelength, demonstrating its superiority in optimization of wirelength.

From the perspectives of the average time and the success rate, ILAm has outstanding performance in terms of the average runtime, which validates that the probabilistic selection strategy for the removal of critical relationships contributes to a fast success of legalization. Meanwhile, the CLA gets legalized floorplans with the shortest runtime, and the significantly smaller HWS D values demonstrate its superior robustness regarding the wirelength of floorplan.

In conclusion, the improved CG-based algorithms (ILAs and ILAm) are capable of generating better floorplans compared to the LA, while the CSAQ-based algorithm can get fast and robust legal floorplans.

### C. Comparison between CSF-qq and other algorithms.

The comparison in Section V-A demonstrates that the Q-learning strategy significantly improves the performance of the CSA-based global floorplanning and legalization, and the competitiveness of the CSAQ-based legalization is also validated in Section V-B. To further verify the performance of the CSA-based fixed-outline floorplanning algorithm assisted by Q-learning, we compare the CSF-qq with some selected floorplanning algorithms, the Parquet-4.5 [3], the Fast-FA [5], the FFA-CD [22] and the Per-RMAP [17]. Among them, Parquet-4.5 and Fast-FA are based on the B\*-tree coding structure of floorplan, and the optimization of wirelength is addressed by the simulated annealing algorithm; FFA-CD utilizes the distribution evolution algorithm based on the probability model to optimize the orientation of modules and employs CSA to optimize the corresponding coordinates of each module to obtain the final solution; Per-RMAP models the floorplanning problem as a feasibility-seeking problem(FSP),

and then deals with the floorplanning problem by introducing a perturbed resettable strategy into the method of alternating projection(MAP). The experiment considers the fixed outline floorplanning of hard modules with a white space setting of  $\gamma = 15\%$ , and the statistical results are shown in Table V. Note that the experimental data of Fast-FA and Per-RMAP are taken from [17], where the success rates are not presented for the benchmark circuits.

TABLE V: Performance Comparison of Selected Fixed-outline Floorplanning Algorithms

Circuit	Method	HPWL( $\mu m$ )	CPU(s)	SR(%)
ami33	Parquet-4.5	78650	0.16	60
	Per-RMAP	63079	0.14	/
	CSF-qq	83665	1.76	100
ami49	Parquet-4.5	962654	0.37	60
	Per-RMAP	689296	1.70	/
	CSF-qq	905653	0.75	100
n100	Parquet-4.5	334719	1.73	100
	Fast-SA	287646	10.72	/
	FFA-CD	293578	0.70	100
	Per-RMAP	282596	1.01	/
	CSF-qq	290156	1.78	100
n200	Parquet-4.5	620097	7.78	100
	Fast-SA	516057	69.86	/
	FFA-CD	521140	1.95	100
	Per-RMAP	518722	2.93	/
	CSF-qq	519211	5.81	100
n300	Parquet-4.5	768747	16.86	100
	Fast-SA	603811	133.63	/
	FFA-CD	588118	3.44	100
	Per-RMAP	626061	4.11	/
	CSF-qq	588866	13.10	100

The numerical results show that, compared with Parquet-4.5, the performance of CSF-qq in optimizing wirelength on GSRC has been improved by 13.3%~23.2%. In addition, CSF-qq far outperforms Fast-SA in terms of running time, and it is also superior in optimizing the wirelength for n300. When compared with the current advanced algorithms FFA-CD and Per-RMAP, CSF-qq remains competitive in both wirelength and running time on GSRC. Finally, we show the fixed-outline floorplanning results of a single independent experiment of CSF-qq on the GSRC benchmarks in Figure 1.

## VI. CONCLUSION

The state-of-the-art researches demonstrate that the analytic floorplanning algorithms generally outperform the counterparts based on the working principle of combinatorial optimization. These analytic floorplanning algorithms typically employ some gradient-based programming algorithms addressing the smoothed objectives, which introduces inevitable distortion to the characteristics of the mathematical model. Consequently, the generated floorplan sometimes is not as optimal as expected.

In this paper, we propose to solve the original nonsmooth objective of floorplanning by the CSA, and the Q-learning strategy is introduced to improve the convergence performance of the CSA-based floorplanning algorithm. Experimental results show that the proposed CSF accelerated by Q-learning (CSF-qq) is competitive to the state-of-the-art fixed-outline floorplanning algorithms in the case that only hard modules are

considered. However, the Q-learning strategy leads to a slight increase on the runtime. Our future work will try to decrease the time complexity of the Q-learning accelerated algorithm, and extend it to the case of large-scale floorplanning with both soft and hard modules.

## REFERENCES

- [1] B. Srinivasan, R. Venkatesan, B. Aljafari, K. Kotecha, V. Indragandhi, and S. Vairavasundaram, "A novel multicriteria optimization technique for vlsi floorplanning based on hybridized firefly and ant colony systems," *IEEE Access*, vol. 11, pp. 14 677–14 692, 2023.
- [2] A. B. Kahng, "Classical floorplanning harmful?" in *Proceedings of the 2000 International Conference on Computer-Aided Design*, ser. ICCAD '00. Washington, DC, USA: IEEE Computer Society Press, 2001, p. 207–213.
- [3] S. N. Adya and I. L. Markov, "Fixed-outline floorplanning: enabling hierarchical design," *IEEE Trans. Very Large Scale Integr. Syst.*, vol. 11, pp. 1120–1135, 2003.
- [4] Y. Weng, Z. Chen, J. Chen, and W. Zhu, "A modified multi-objective simulated annealing algorithm for fixed-outline floorplanning," in *2018 IEEE International Conference on Automation, Electronics and Electrical Engineering (AUTEEL)*, 2018, pp. 35–39.
- [5] T.-C. Chen and Y.-W. Chang, "Modern floorplanning based on B\*-tree and fast simulated annealing," *IEEE Transactions on Computer-Aided Design of Integrated Circuits and Systems*, vol. 25, no. 4, pp. 637–650, 2006.
- [6] J. Chen and W. Zhu, "A hybrid genetic algorithm for VLSI floorplanning," in *2010 IEEE International Conference on Intelligent Computing and Intelligent Systems*, vol. 2, 2010, pp. 128–132.
- [7] D. Zou, G. Wang, G. Pan, and H. Qi, "A modified simulated annealing algorithm and an excessive area model for floorplanning using fixed-outline constraints," *Frontiers of Information Technology & Electronic Engineering*, vol. 17, no. 11, pp. 1228–1244, 2016.
- [8] Y. Ye, X. Yin, Z. Chen, Z. Hong, X. Fan, and C. Dong, "A novel method on discrete particle swarm optimization for fixed-outline floorplanning," in *2020 IEEE International Conference on Artificial Intelligence and Information Systems (ICAIS)*, 2020, pp. 591–595.
- [9] J. Z. Yan and C. Chu, "Defer: Deferred decision making enabled fixed-outline floorplanning algorithm," *IEEE Transactions on Computer-Aided Design of Integrated Circuits and Systems*, vol. 29, no. 3, pp. 367–381, 2010.
- [10] P. Ji, K. He, Z. Wang, Y. Jin, and J. Wu, "A Quasi-Newton-based floorplanner for fixed-outline floorplanning," *Computers & Operations Research*, vol. 129, p. 105225, 2021.
- [11] Z. Huang, X. Li, and W. Zhu, "Optimization models and algorithms for placement of very large scale integrated circuits," *Operations Research Transactions*, vol. 25, no. 3, pp. 15–36, 2021.
- [12] X. Li, K. Peng, F. Huang, and W. Zhu, "Pef: Poisson's equation-based large-scale fixed-outline floorplanning," *IEEE Transactions on Computer-Aided Design of Integrated Circuits and Systems*, vol. 42, no. 6, pp. 2002–2015, 2023.
- [13] F. Huang, D. Liu, X. Li, B. Yu, and W. Zhu, "Handling orientation and aspect ratio of modules in electrostatics-based large scale fixed-outline floorplanning," in *2023 IEEE/ACM International Conference on Computer Aided Design (ICCAD)*, 2023, pp. 1–9.
- [14] Y. Zhan, Y. Feng, and S. Sapatnekar, "A fixed-die floorplanning algorithm using an analytical approach," in *Asia and South Pacific Conference on Design Automation, 2006.*, 2006, pp. 6 pp.–.
- [15] J.-M. Lin and Z.-X. Hung, "UFO: Unified convex optimization algorithms for fixed-outline floorplanning considering pre-placed modules," *IEEE Transactions on Computer-Aided Design of Integrated Circuits and Systems*, vol. 30, no. 7, pp. 1034–1044, 2011.
- [16] J. Lu, P. Chen, C.-C. Chang, L. Sha, D. J.-H. Huang, C.-C. Teng, and C.-K. Cheng, "ePlace: Electrostatics-based placement using fast fourier transform and nesterov's method," *ACM Trans. Des. Autom. Electron. Syst.*, vol. 20, no. 2, Mar. 2015.
- [17] S. Yu, Y. Censor, and G. Luo, "Floorplanning with I/O assignment via feasibility-seeking and superiorization methods," *IEEE Transactions on Computer-Aided Design of Integrated Circuits and Systems*, vol. 44, no. 1, pp. 317–330, 2025.
- [18] Y.-W. Chang, Z.-W. Jiang, and T.-C. Chen, "Essential issues in analytical placement algorithms," *IPSSJ Trans. Syst. LSI Des. Methodol.*, vol. 2, pp. 145–166, 2009.

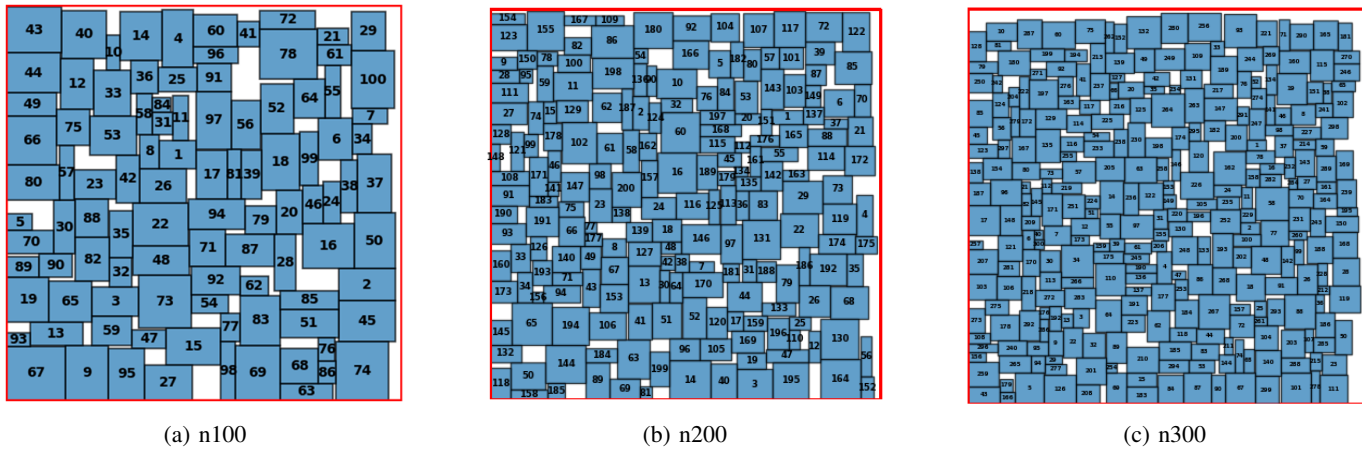


Fig. 1: The Floorplans of GSRC benchmarks generated by CSF-qq.

- [19] B. Ray and S. Balachandran, "An efficient wirelength model for analytical placement," in *2013 Design, Automation & Test in Europe Conference & Exhibition (DATE)*, 2013, pp. 1711–1714.
- [20] T. F. Chan, J. Cong, J. R. Shinnerl, K. Sze, and M. Xie, "mPL6: enhanced multilevel mixed-size placement," in *Proceedings of the 2006 International Symposium on Physical Design*, ser. ISPD '06. New York, NY, USA: Association for Computing Machinery, 2006, p. 212–214.
- [21] W. Zhu, J. Chen, Z. Peng, and G. Fan, "Nonsmooth optimization method for VLSI global placement," *IEEE Transactions on Computer-Aided Design of Integrated Circuits and Systems*, vol. 34, no. 4, pp. 642–655, 2015.
- [22] J. Sun, H. Cheng, J. Wu, Z. Zhu, and Y. Chen, "Floorplanning of VLSI by mixed-variable optimization," in *Intelligence Computation and Applications*, K. Li and Y. Liu, Eds. Singapore: Springer Nature Singapore, 2024, pp. 137–151.
- [23] Z. He, Y. Ma, L. Zhang, P. Liao, N. Wong, B. Yu, and M. D. Wong, "Learn to floorplan through acquisition of effective local search heuristics," in *2020 IEEE 38th International Conference on Computer Design (ICCD)*, 2020, pp. 324–331.
- [24] A. Mirhoseini, A. Goldie, M. Yazgan *et al.*, "A graph placement methodology for fast chip design," *Nature*, vol. 594, pp. 207–212, 2021.
- [25] Q. Xu, H. Geng, S. Chen, B. Yuan, C. Zhuo, Y. Kang, and X. Wen, "Goodfloorplan: Graph convolutional network and reinforcement learning-based floorplanning," *IEEE Transactions on Computer-Aided Design of Integrated Circuits and Systems*, vol. 41, no. 10, pp. 3492–3502, 2022.
- [26] B. Yang, Q. Xu, H. Geng, S. Chen, and Y. Kang, "Miracle: Multi-action reinforcement learning-based chip floorplanning reasoner," in *2024 Design, Automation & Test in Europe Conference & Exhibition (DATE)*, 2024, pp. 1–6.
- [27] C. Watkins and P. Dayan, "Q-learning," *Machine Learning* 8, pp. 279–292, 1992.
- [28] J. Qin, M. Li, Y. Shi, Q. Ma, and W. X. Zheng, "Optimal synchronization control of multiagent systems with input saturation via off-policy reinforcement learning," *IEEE Transactions on Neural Networks and Learning Systems*, vol. 30, no. 1, pp. 85–96, 2019.
- [29] H. Li, K. Gao, P.-Y. Duan, J.-Q. Li, and L. Zhang, "An improved artificial bee colony algorithm with q-learning for solving permutation flow-shop scheduling problems," *IEEE Transactions on Systems, Man, and Cybernetics: Systems*, vol. 53, no. 5, pp. 2684–2693, 2023.